Abdominal Radiology

Published online: 30 August 2017

Abdom Radiol (2018) 43:880–898
https://doi.org/10.1007/s00261-017-1307-0

Applications of contrast-enhanced ultrasound in the kidney

Brittany Kazmierski, Corinne Deurdulian, Hisham Tchelepi, Edward G. Grant

Department of Radiology, Keck USC School of Medicine, 1500 San Pablo Street, 2nd Floor Imaging, Los Angeles, CA 90033, USA

Abstract

Incidental discovery of renal lesions on cross-sectional imaging studies performed for other indications is not uncommon. With the increased reliance on medical imaging, the number of incidentally detected renal lesions has also grown over time. While simple cysts account for the majority of these lesions, the presence of complex features within a cystic lesion, such as septations and solid components, can present a confusing picture. Solid lesions, too, can be indeterminate, and distinguishing between benign solid masses (like lipid-poor angiomyolipomas and oncocytomas) and renal cell carcinoma affects patient management and can prevent unnecessary interventions. Indeterminate renal lesions are traditionally further characterized by multiphase imaging, such as contrast-enhanced computed tomography and magnetic resonance imaging. Contrast-enhanced ultrasound (CEUS) is a new, relatively inexpensive technique that has become increasingly employed in the diagnostic workup of indeterminate renal lesions. With its lack of nephrotoxicity, the absence of ionizing radiation, and the ability to evaluate the enhancement pattern of renal lesions quickly and in real-time, CEUS has unique advantages over traditional imaging modalities. This article provides an overview of the current clinical applications of CEUS in characterizing renal lesions, both cystic and solid. Additional applications of CEUS in the kidney, including its roles in renal transplant evaluation and guidance for percutaneous biopsy, will also be briefly discussed.

Key words: Contrast-enhanced ultrasound—Renal cyst—Renal mass—Renal cell carcinoma—Angiomyolipoma—Oncocytoma

Electronic supplementary material The online version of this article (doi:10.1007/s00261-017-1307-0) contains supplementary material, which is available to authorized users.

Correspondence to: Brittany Kazmierski; *email:* brittany.kazmierski@med.usc.edu

Overview of contrast-enhanced ultrasound

Characterization of indeterminate renal lesions is typically achieved by multiphase contrast-enhanced CT (CECT) and MRI. Contrast-enhanced ultrasound (CEUS) is a relatively new technique that has demonstrated much promise in the workup of renal lesions (Table 1). The contrast agents employed in CEUS comprise tiny microbubbles of gas surrounded by a stabilizing shell. The microbubbles have poor solubility within the blood and are eliminated through the lungs via respiration, while the stabilizing shell is metabolized by the body. These elimination properties make CEUS a particularly attractive non-toxic imaging modality for patients with a history of chronic renal insufficiency, dialysis, kidney transplant, and nephrectomy. Additionally, in the case of renal lesions, the lack of renal excretion prevents obscuration or confounding of a lesion's enhancement pattern by collecting system enhancement. Other advantages of CEUS include the ability to observe and record a lesion's enhancement in real-time, in contrast to the static images obtained at set time points with CT and MRI. CEUS is relatively inexpensive, does not utilize ionizing radiation, and can be completed quickly, with the decision to perform CEUS often being made immediately following a patient's diagnostic ultrasound scan. Furthermore, because CEUS is performed at the bedside, it is a useful imaging modality in children and claustrophobic patients who cannot tolerate CT or MRI without sedation.

Commercially available ultrasound scanners with contrast-specific software are employed for all examinations. Typically, a C5-1 curved array abdominal transducer is used. Baseline pre-contrast assessment of the bilateral renal parenchyma and collecting system is performed. Since, in most cases, a previously identified lesion is to be further assessed with contrast, prior imaging is reviewed and optimal views of the lesion in question are obtained using grayscale technique. The ultrasound scanner is then switched to contrast mode and the agent

Table 1. Enhancement pattern of solid renal masses relative to the renal cortex on CEUS

Solid lesion	Arterial	Venous	Delayed
Clear cell renal cell carcinoma	Hyperenhancing	Early washout	Continued washout
Papillary renal cell carcinoma	Hypoenhancing	Hypoenhancing	Hypoenhancing
Angiomyolipoma	Variable	Variable	Variable
Oncocytoma	Variable	Variable	Variable
Pseudotumor	Isoenhancing	Isoenhancing	Isoenhancing
Pyelonephritis	Hypoenhancing	Hypoenhancing	Hypoenhancing
Renal abscess	Non-enhancing	Non-enhancing	Non-enhancing
Metastasis/lymphoma	Hypoenhancing	Hypoenhancing	Hypoenhancing

administered. At our institution, we use low MI scanning with a dual screen display. Half of the screen is displayed in conventional grayscale mode to localize the lesion, and pulse inversion/harmonic imaging is used in the other half to optimally obtain contrast-enhanced images. Ideally, one should include images of the lesion and of at least some of the surrounding renal parenchyma for comparison. Contrast injection typically consists of a 1.5 mL dose of Lumason injected intravenously, which is followed immediately by a flush of 10 mL of normal saline. Continuous imaging of the area in question is normally carried out for a period of 3–5 min following injection. Repeat injections are administered after the contrast dissipates, if necessary.

Case presentation

Solid renal cell carcinoma

Renal cell carcinoma (RCC) is the most prevalent primary renal malignancy, with clear cell RCC representing the most common subtype. Between 1983 and 2002, the incidence of RCC increased from 7.1 to 10.8 cases per 100,000 patients, and the mortality increased from 1.5 to 6.5 deaths per 100,000 patients in that same timeframe [1]. Differentiating RCC from other solid renal masses, both benign and malignant, has important implications for patient treatment and prognosis. Benign solid renal lesions include angiomyolipoma (AML) and oncocytoma. Non-RCC malignant renal neoplasms include lymphoma, transitional cell carcinoma, and metastatic disease.

On traditional multiphase CECT imaging, there is some variability in the enhancement pattern of RCC based on subtype. Jinzaki et al. reported that clear cell RCC, the most common variant, frequently demonstrates heterogeneous enhancement that is hyperenhancing to the renal parenchyma in the corticomedullary phase and becomes hypoenhancing in the nephrographic phase [2]. Chromophobe RCC also demonstrates peak enhancement in the corticomedullary phase, but to a lesser degree than with clear cell RCC. Papillary RCC demonstrates gradual, progressive enhancement and is typically hypoenhancing relative to the other RCC subtypes, which can make distinguishing this lesion from a benign entity such as oncocytoma difficult.

Common characteristics of clear cell RCC with CEUS include heterogeneous avid early enhancement, a peripheral rim of enhancement (pseudocapsule), and early washout (Figs. 1, 2). Papillary RCC typically remains hypoenhancing to the renal cortex on all phases (Fig. 3), similar to the enhancement pattern seen on CT. Li et al. reported that 76.5% of RCCs were hyperenhancing to the background renal parenchyma in the cortical phase (defined as 8–35 s following contrast injection) and 10.6% were isoenhancing [3]. In the late phase (defined as >120 s following contrast injection), 84.7% of RCCs were hypoenhancing. Larger lesions (>4 cm) were more heterogeneously enhancing than smaller lesions, and the majority of RCCs showed a pseudocapsule in the cortical phase. When the evaluated RCCs were subdivided by histological subtype, the papillary and chromophobe subtypes showed a lesser degree of enhancement in the cortical phase than clear cell RCC.

Xu et al. evaluated 84 RCCs by CEUS. They found that 88.1% of RCCs showed hyperenhancement in the cortical phase [4]. Of those lesions, 73.4% became hypoenhancing to the renal parenchyma in the corticomedullary phase, while the others remained hyperenhancing or isoenhancing. Larger tumors (>3 cm) were shown to be more heterogeneously enhancing than smaller lesions. A study by Barr et al. also showed an arterial enhancement and delayed washout pattern with RCC [5].

Additional characterization of solid RCC can be achieved by producing a time–intensity curve. CEUS technique allows for continuous evaluation of the kidney following contrast administration, with storage of the images as a cine clip. The images can be post-processed to generate a graphical, quantitative depiction of a lesion's enhancement pattern, which is then compared to adjacent normal renal cortex. This can be helpful in differentiating solid renal masses. A study by King et al. looked at the enhancement pattern of solid renal masses utilizing time–intensity curve analysis [6]. In the case of RCC, they found that the clear cell subtype had greater peak intensity than the renal cortex, as well as a shorter time to peak intensity (Fig. 4A), while the de-enhancement features were

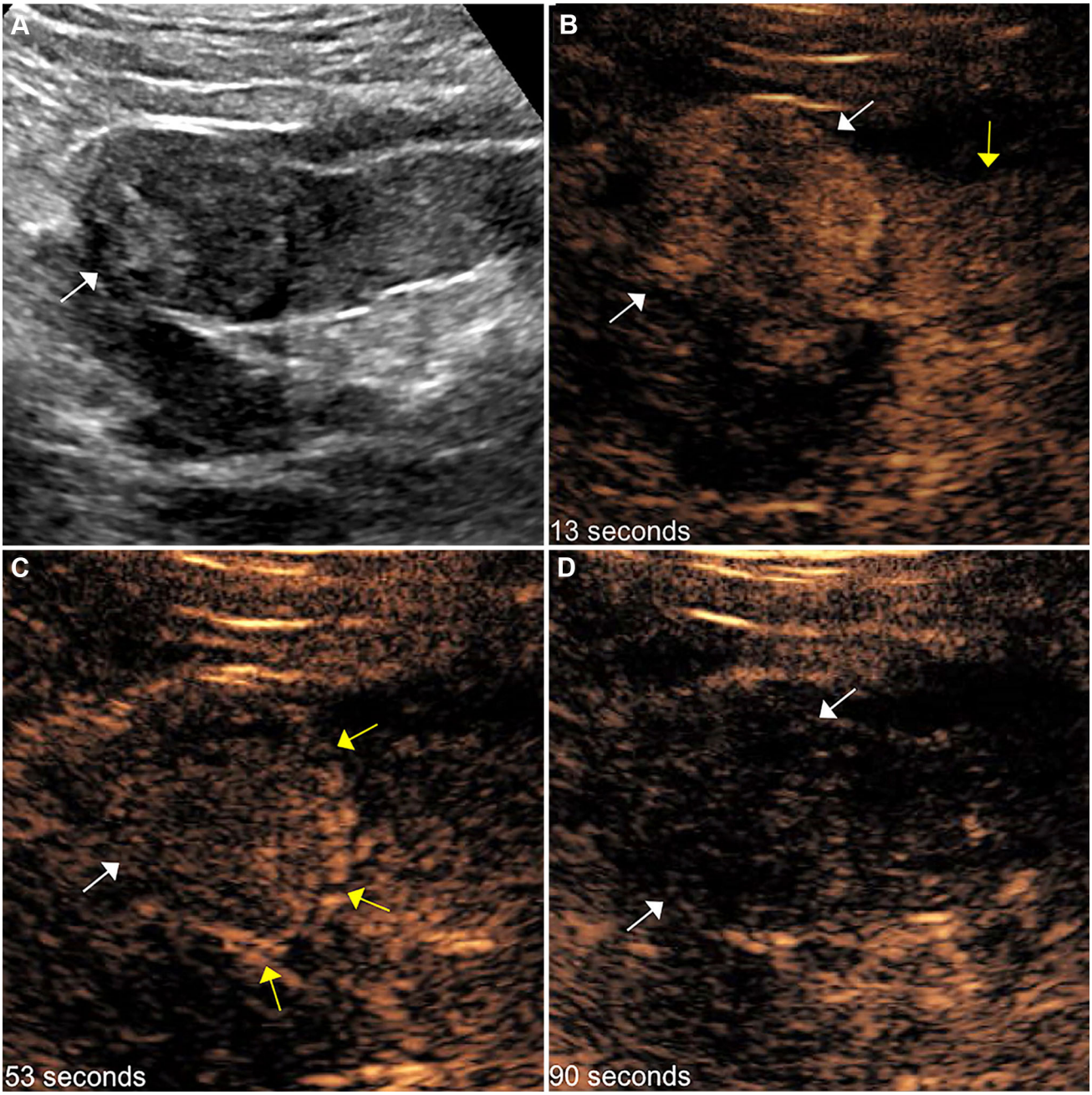

Fig. 1. A 51-year-old male with solid left renal mass. **A** Grayscale sonographic image of the left kidney demonstrates an oval isoechoic mass at the upper pole (*arrow*). **B** CEUS in the arterial phase (13 s) shows avid arterial enhancement of this lesion (*white arrows*) greater than the adjacent renal cortex (*yellow arrow*). **C** In the venous phase (53 s), there is washout of this lesion (*white arrow*) with a thin pseudocapsule apparent (*yellow arrows*). **D** Delayed phase image (90 s) shows continued washout of the lesion (*arrows*). This mass was diagnosed as clear cell RCC at percutaneous core needle biopsy.

variable. This pattern was in contrast to that of papillary RCC, which enhanced later than clear cell RCC and remained hypoenhancing to the renal cortex (Fig. 4B). Chromophobe RCC demonstrated an intermediate enhancement pattern, similar to the renal cortex (Fig. 4C).

Complex cystic lesions

Incidental cystic lesions are frequently encountered within the kidney and are increasingly common in older patient populations, being found in approximately 50% of patients aged over 50 years [7]. These can range from a

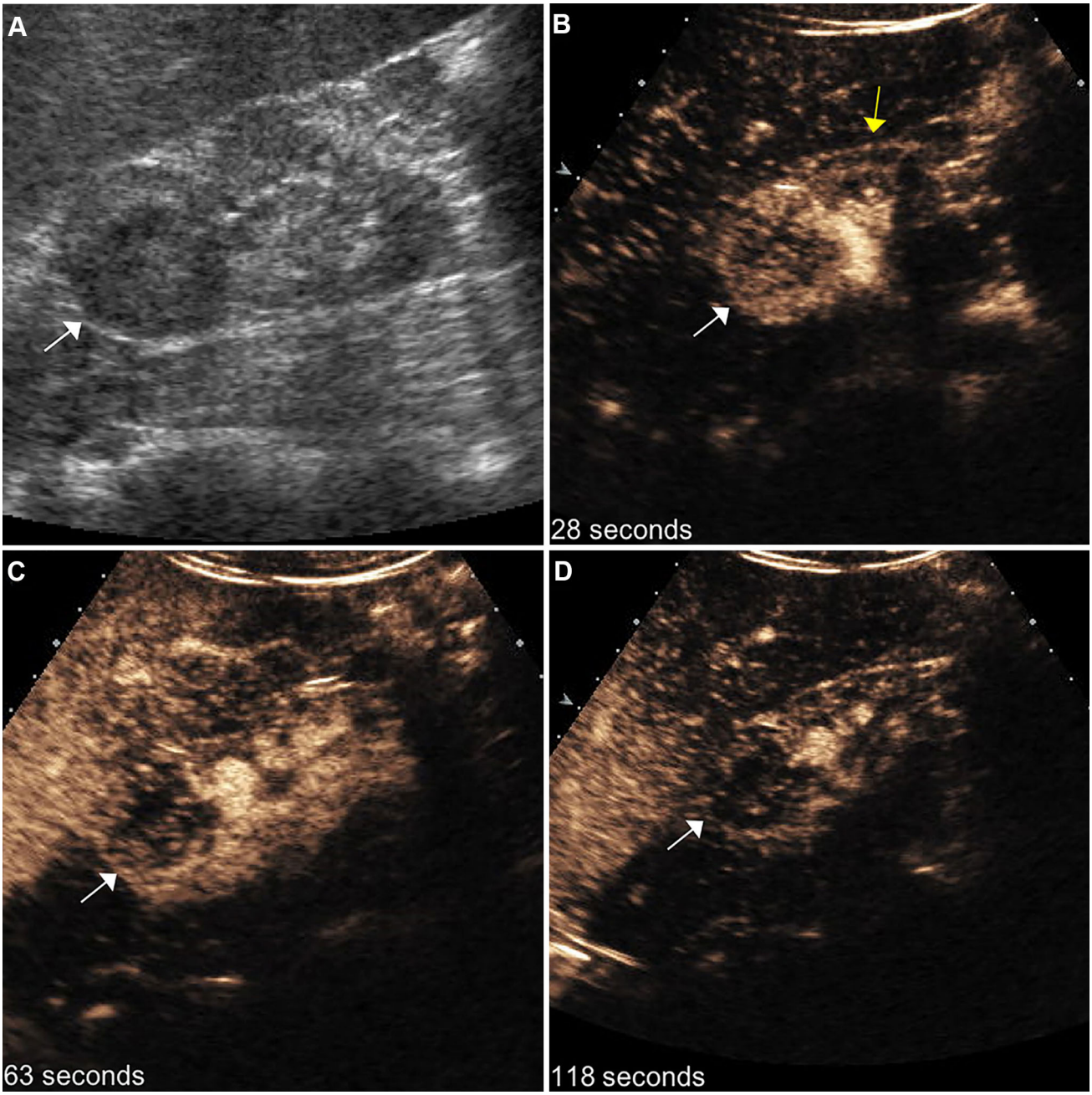

Fig. 2. A 51-year-old male with end-stage renal disease (creatinine 5.8) and solid right renal mass detected on non-contrast CT. **A** Grayscale ultrasound image shows a solid hypoechoic mass at the right renal upper pole (*arrow*). **B** CEUS in the arterial phase (28 s) reveals early enhancement of this mass (*white arrow*) greater than the background renal parenchyma (*yellow arrow*). **C** In the venous phase (63 s), this mass begins to demonstrate washout (*arrow*). **D** In the delayed phase (118 s), there is continued washout of this mass (*arrow*) relative to the renal cortex. This enhancement pattern is typical of clear cell RCC.

benign simple cyst with negligible malignant potential to a complex cystic lesion with suspicious features. Cystic lesions detected on CT are typically characterized using the Bosniak classification system, which was initially published in 1986 and has undergone several revisions over time [8]. The Bosniak system aims to classify renal lesions seen on CECT based on the presence of certain features that may affect the likelihood that the lesion is malignant. Imaging characteristics that increase a lesion's Bosniak score include hyperdensity, septations, calcifications, wall thickening, and enhancing nodular or solid components. A higher Bosniak score corresponds to an increased likelihood of malignancy for a particular lesion.

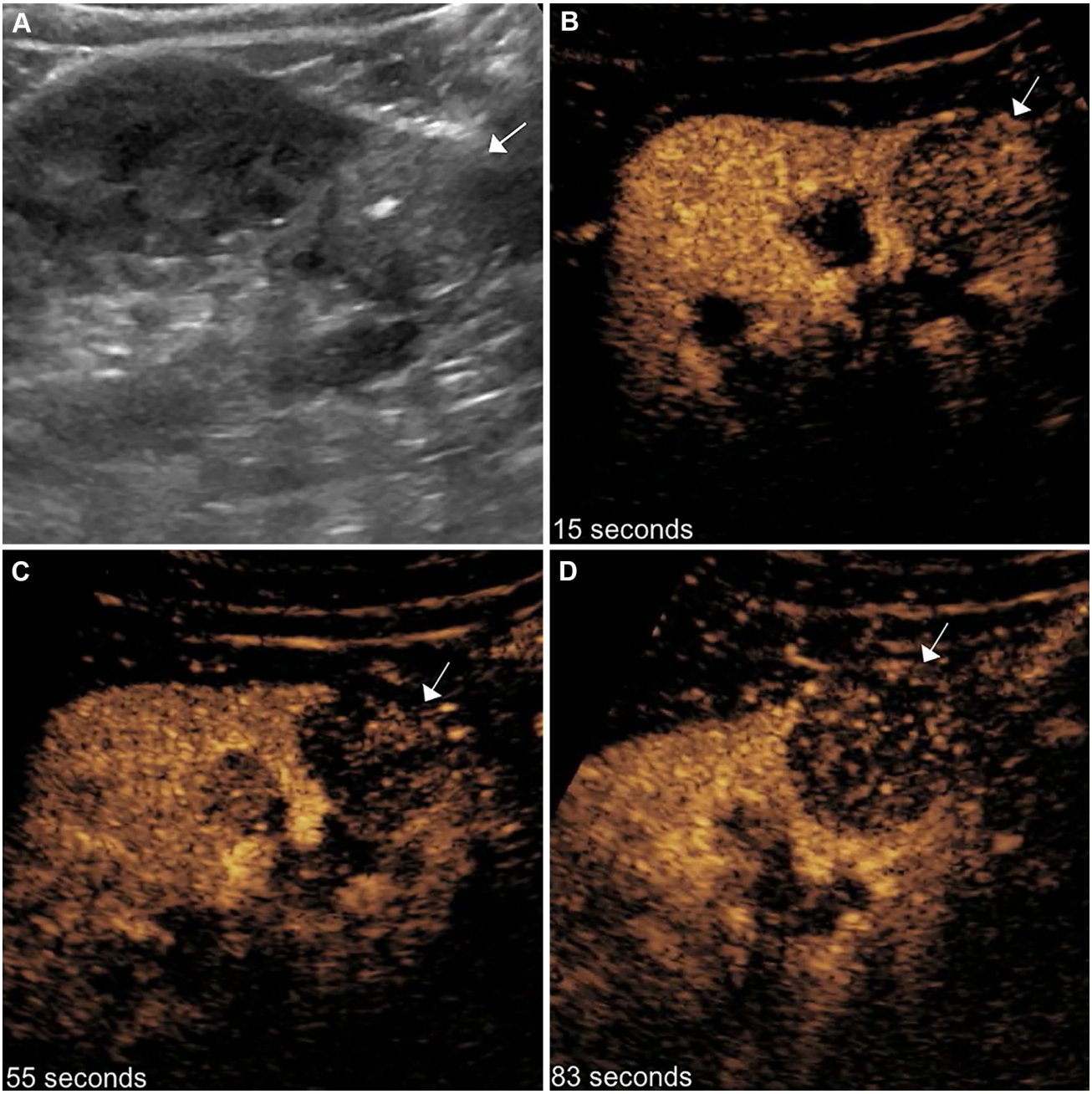

Fig. 3. A 61-year-old male with left renal mass. **A** Grayscale sonographic image demonstrates a mildly hyperechoic mass at the left renal lower pole (*arrow*) with a coarse internal calcification. **B** CEUS in the arterial phase (15 s) shows this mass to be hypoenhancing (*arrow*) relative to the renal cortex. **C** This mass remains hypoenhancing (*arrow*) in the venous phase (55 s). **D** In the delayed phase (83 s), the mass continues to hypoenhance (*arrow*). This enhancement pattern is typical of papillary RCC, though benign masses can have a similar appearance.

CECT is often the initial imaging modality utilized in characterizing cystic renal lesions. RCC can occasionally manifest as a complex cystic lesion, though this is not its most common presentation. For this reason, multiphase CT (including pre-contrast, arterial phase, and nephrographic phase images) is commonly employed to further characterize indeterminate complex cystic renal lesions. The presence of irregular calcifications, thickened septations, and enhancing nodular components are all features that can be seen within a complex cystic lesion, benign or malignant [9]. MRI can provide additional information about the nature of a cystic renal lesion. Intrinsic high T1 signal intensity within a lesion suggests the presence of lipid, blood products, or proteinaceous material. Contrast-enhanced MR yields similar information to CT, although it has been shown to be more

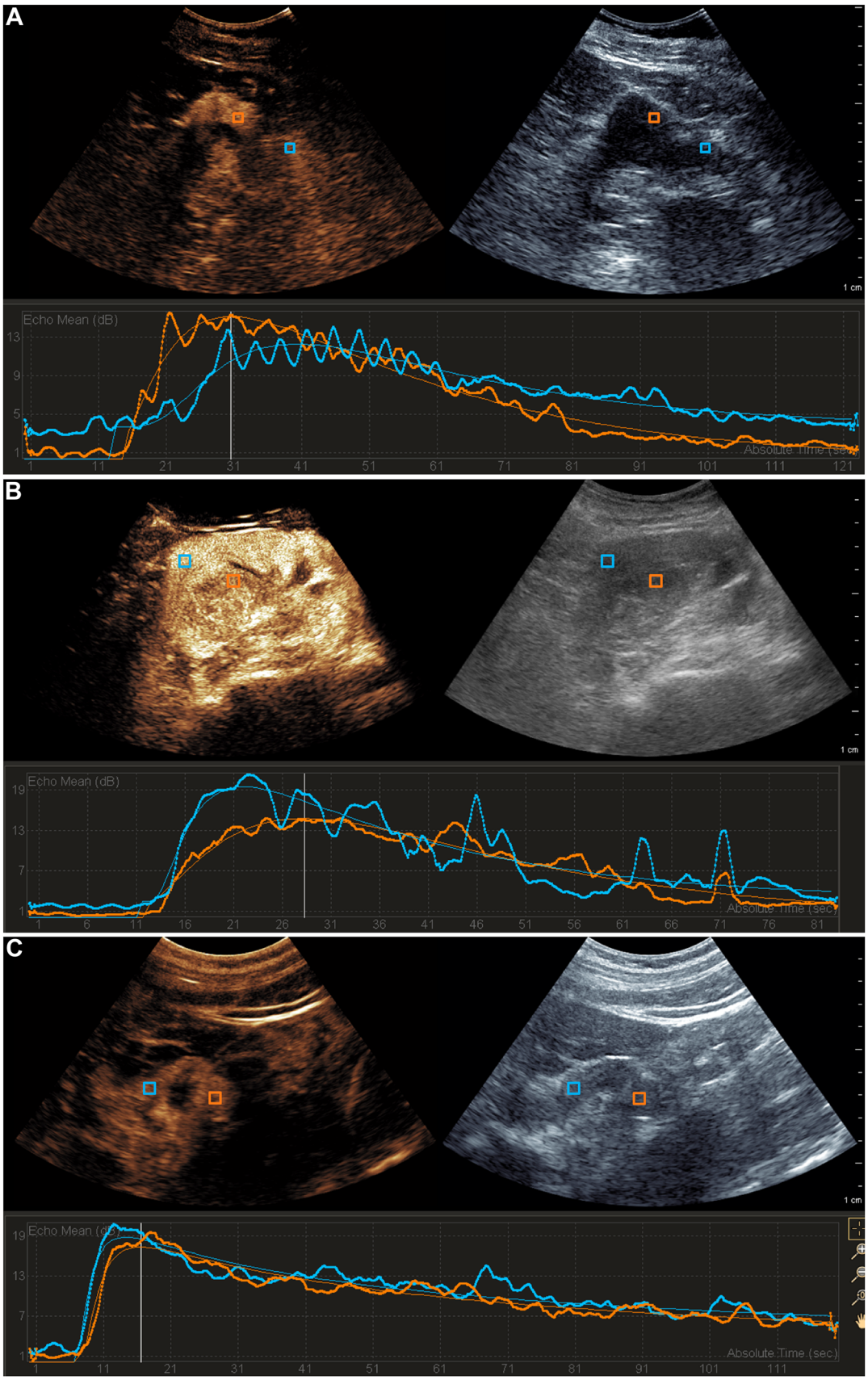
A
1 cm
Echo Mean (dB)
13
9
5
1
1 11 21 31 41 51 61 71 81 91 101 111 121
Absolute Time (sec)
B
1 cm
Echo Mean (dB)
19
13
7
1
1 6 11 16 21 26 31 36 41 46 51 56 61 66 71 76 81
Absolute Time (sec)
C
1 cm
19
13
7
1
1 11 21 31 41 51 61 71 81 91 101 111
Absolute Time (sec)

◀**Fig. 4.** CEUS images with time–intensity curves for multiple types of RCC. **A** Clear cell RCC characteristically demonstrates avid arterial enhancement (*orange curve*), earlier and to a greater degree than the renal cortex (*blue curve*). In this case, the tumor demonstrates eventual washout, but the delayed enhancement characteristics of clear cell RCC are variable. **B** Papillary RCC demonstrates a slower time to peak enhancement than the renal cortex and is typically hypoenhancing on all phases. **C** Chromophobe RCC usually demonstrates less enhancement than clear cell RCC, but greater enhancement than papillary RCC. The enhancement pattern is very similar to the adjacent normal renal cortex, with peak tumor enhancement being only slightly less than the cortex. Images courtesy of Dr. Kevin King of the Keck USC School of Medicine, Department of Radiology.

sensitive in identifying septations, evaluating the degree of septal thickening, and detecting enhancement within a lesion [10].

Ultrasound is an excellent modality for evaluating cystic renal lesions. A benign simple cyst is well-circumscribed, completely anechoic, smoothly marginated, and has a well-defined backwall with increased through transmission. The presence of internal debris, septations, wall thickening, shadowing calcifications, and solid components within a cyst are features that indicate complexity. Color and power Doppler can be used to evaluate vascularity within septations and solid components, but Doppler may fail to detect slow vascular flow and small blood vessels.

Further characterization of cystic renal lesions is a frequent application of CEUS. The use of ultrasound contrast agents can reveal whether a complex cystic lesion's septations demonstrate enhancement (Figs. 5, 6). In a study by Park et al. CEUS resulted in upgrading the Bosniak score in 26% of cystic renal lesions that had been previously classified by CECT [11]. CEUS detected a higher number of septations within a lesion than CECT. It also was superior in detecting the degree of septal wall thickening, septal enhancement, and enhancement of solid components within the lesion. Quaia et al. demonstrated superior diagnostic accuracy of CEUS when compared with CECT and conventional ultrasound [12]. Ascenti et al. showed that CEUS was more sensitive than CT for detection of intralesional septations and enhancement [13].

However, it is important to note that CEUS has superior temporal and spatial resolution when compared to other imaging modalities, and the significance of vascular flow within septations is uncertain [14]. The Bosniak criteria were originally developed for cystic lesions seen on CT [8]. CEUS inherently demonstrates more complexity in cystic lesions due to improved signal-to-noise ratio, and one should use caution when applying Bosniak criteria to CEUS findings. As with CECT and MRI, the presence of enhancement within frankly nodular and solid components on CEUS should raise suspicion for malignancy (Fig. 7).

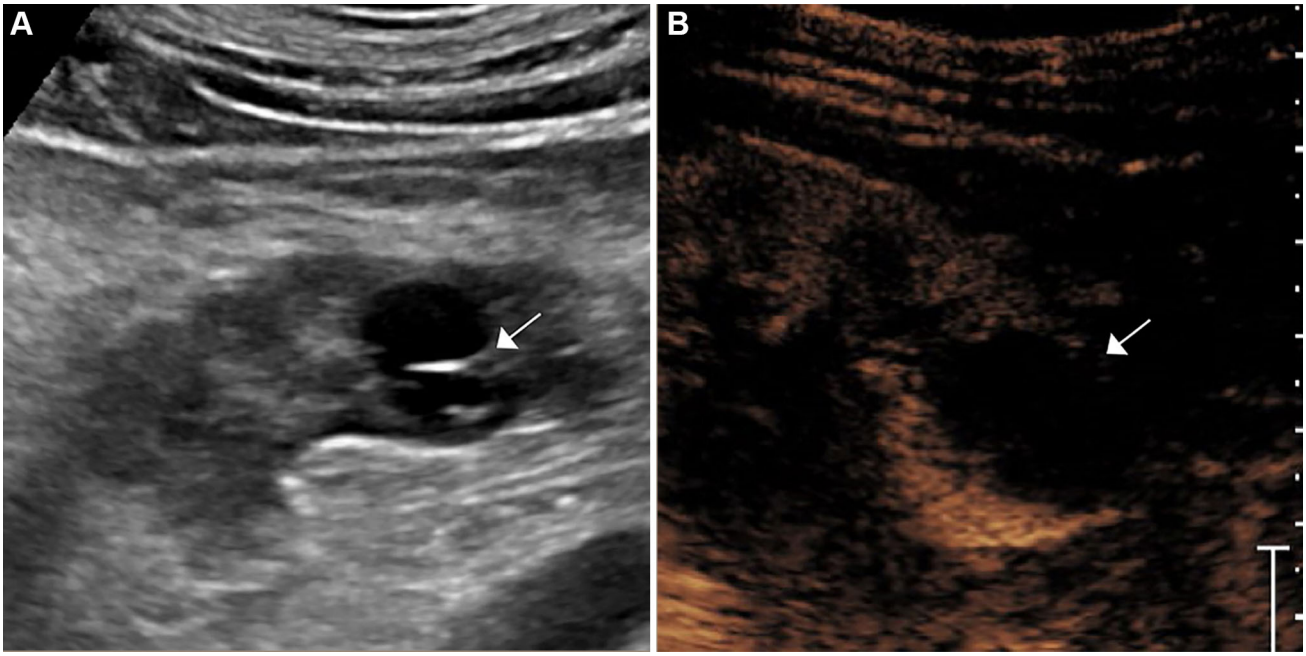

Fig. 5. A 78-year-old man with a history of renal insufficiency and a complex left renal cyst. **A** Grayscale sonographic image of the left kidney demonstrates a cystic lesion at the left renal lower pole with internal septations (*arrow*). **B** CEUS image shows no internal enhancement within the cyst septations (*arrow*). This is consistent with a benign septated cyst.

Angiomyolipoma

Renal AMLs are benign, fat-containing solid mesenchymal tumors that are commonly encountered in abdominal imaging. They comprise adipose, smooth muscle, and aberrant blood vessels. They are typically asymptomatic, but larger AMLs (>4 cm) are at risk for hemorrhage due to the more prominent vascular components. AMLs have a female predominance. While the majority of AMLs occur sporadically, there is an association with genetic syndromes like the tuberous sclerosis complex (TSC) and lymphangioleiomyomatosis (LAM).

Given that the vast majority of AMLs contain macroscopic fat, they most commonly present as a uniformly hyperechoic lesion on conventional ultrasound. However, there can be variability in the intralesional fat content of an AML, and lipid-poor AMLs can have an isoechoic or mildly hyperechoic sonographic appearance. Furthermore, RCC can be uniformly hyperechoic on ultrasound and mimic the appearance of an AML. Forman et al. demonstrated that 32% of small renal tumors (<3 cm in diameter) were sufficiently hyperechoic to mimic an AML [15].

Additional characterization of hyperechoic renal lesions with multiphase cross-sectional imaging can aid in the diagnosis of AML, as macroscopic fat will be negative in attenuation on CT and demonstrate signal dropout on fat-suppressed MR sequences. Opposed-phase MR imaging can show a low signal intensity rim at the interface between an AML and the adjacent renal parenchyma due to chemical shift artifact. However, these features may be absent in lipid-poor AMLs. Jinzaki et al. reported that approximately 4.5% of AMLs are lipid-poor due to an abundance of smooth muscle components [16]. These lesions were higher in attenuation than fat on non-contrast CT, enhanced homogeneously on CECT, and were isoechoic on ultrasound.

The enhancement pattern of an AML on CEUS can be variable. The study by Xu et al. showed no significant difference in the degree or timing of enhancement between AMLs and RCCs during the cortical phase (8–35 s after contrast injection) [17]. However, most of

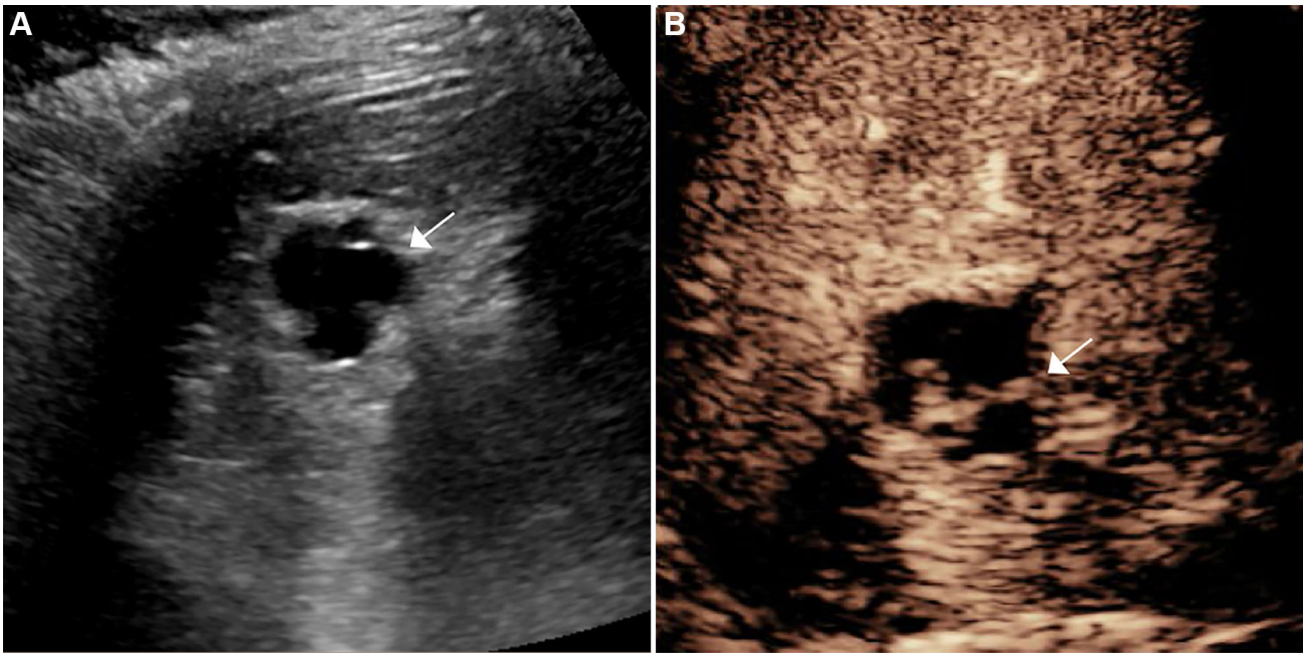

Fig. 6. A 75-year-old female with a history of complex right renal cyst. **A** Grayscale sonographic image of the right kidney demonstrates a complex renal cyst with internal septations at the upper pole (*arrow*). **B** CEUS shows multiple thickened, enhancing internal septations (*arrow*). As this patient is a poor surgical candidate, she will have a 6-month follow-up CEUS to assess for stability.

Fig. 7. A 68-year-old female with chronic renal insufficiency and a left renal complex cystic lesion. **A** T2-weighted MR image demonstrates a complex cystic lesion at the left renal upper pole (*white arrow*) with multiple internal septations and a central nodular component (*black arrow*). **B** Grayscale image of the left kidney shows a large, septated cystic mass with solid components (*arrows*). **C** CEUS obtained during the arterial phase (27 s) reveals avid enhancement of the solid components (*arrow*) greater than the background renal cortex. **D** In the venous phase (55 s), the solid components begin to demonstrate washout (*arrow*). **E** This washout (*arrow*) continues into the delayed phase (89 s). This lesion was diagnosed as clear cell RCC following robotic left partial nephrectomy.

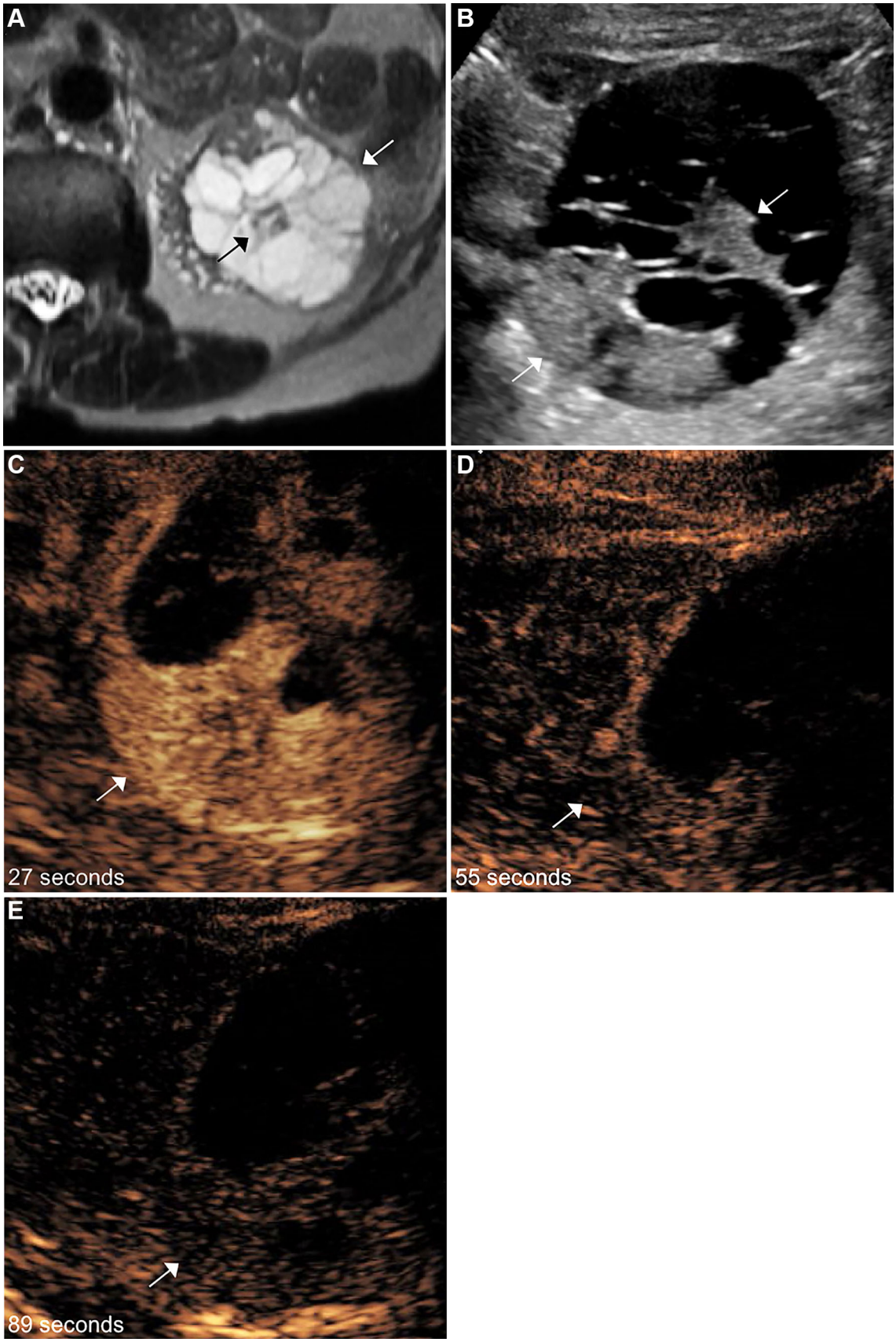
A
B
C
27 seconds
D
55 seconds
E
89 seconds

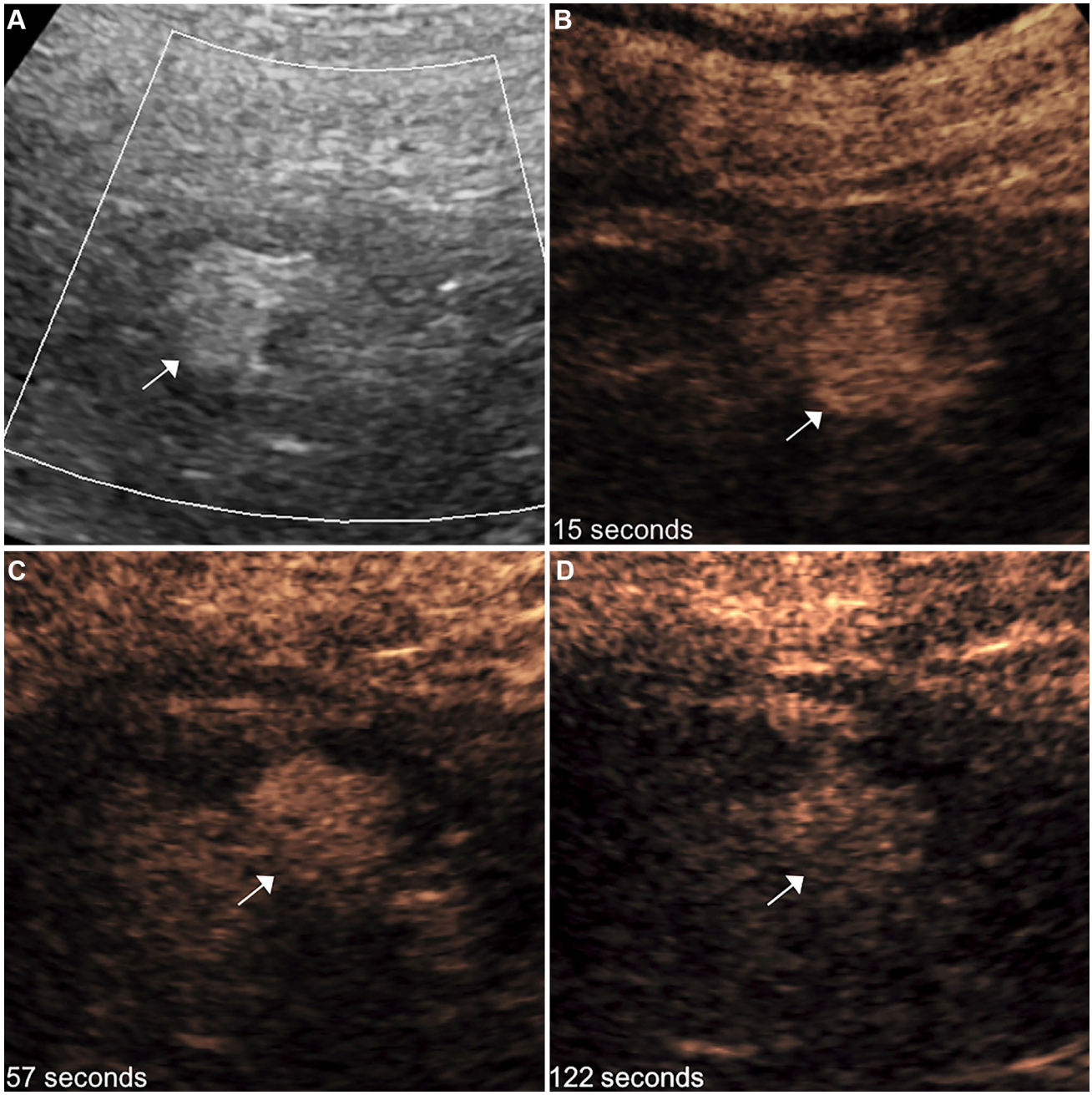

Fig. 8. An 83-year-old female with a solid right renal lesion. **A** Color Doppler image of the right kidney reveals a hyperechoic lesion at the upper pole (*arrow*) without demonstrable internal vascularity. **B** CEUS obtained during the arterial phase (15 s) demonstrates early enhancement of this lesion greater than the background renal parenchyma (*arrow*). **C** Enhancement of this lesion persists (*arrow*) in the venous phase (57 s). **D** Delayed phase image (122 s) demonstrates persistent faint enhancement (*arrow*). This lesion represented an AML, but note that the enhancement pattern of AML can be variable.

the evaluated RCCs demonstrated hypoenhancement in the corticomedullary (36–120 s after contrast injection) and delayed (>120 s after contrast injection) phases. Conversely, 78.8% of AMLs demonstrated sustained hyperenhancement or isoenhancement in these phases (Fig. 8). The majority of AMLs showed uniform enhancement, as compared to the heterogeneous enhancement pattern of RCCs. However, Barr et al. reported that all 61 AMLs included in the study demonstrated contrast enhancement less than that of the adjacent renal cortex [5]. This was in contrast to echogenic RCCs, which all demonstrated arterial enhancement and delayed washout. As there is considerable overlap in the imaging features of AML and RCC, CEUS should not be used alone to discriminate between these two lesions.

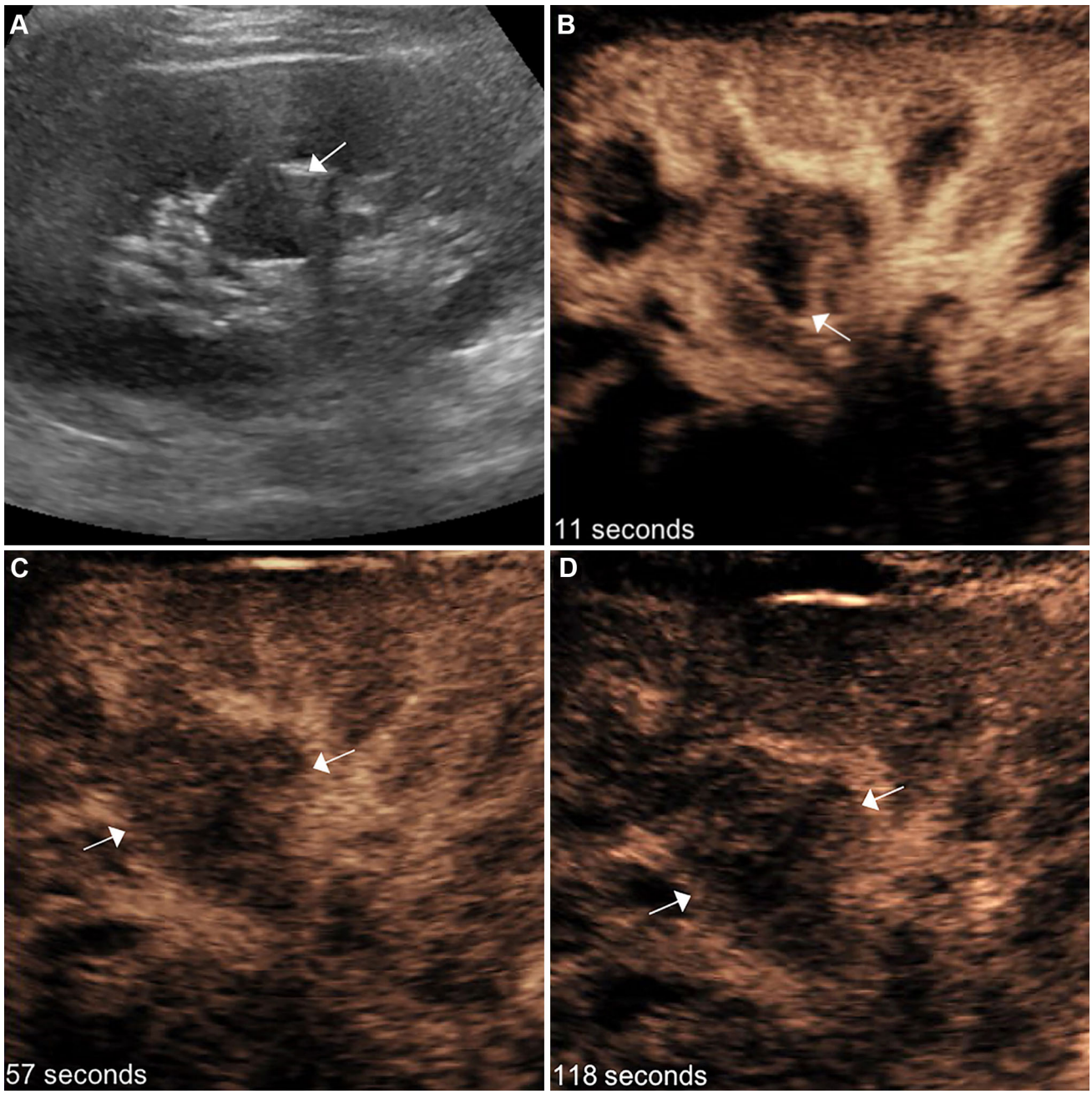

Fig. 9. A 21-year-old female with left renal mass-like area noted on ultrasound. **A** Grayscale sonographic image of the left kidney demonstrates a hypoechoic structure projecting into the renal sinus fat that is similar in echogenicity to the renal cortex (*arrow*). **B** CEUS in the early arterial phase (11 s) reveals that this structure has similar enhancement to the renal cortex and contains a central medullary pyramid (*arrow*). **C** Venous phase image (57 s) shows continued enhancement similar to the renal cortex (*arrows*). **D** Isoenhancement persists in the delayed phase (118 s), with no discrete mass lesion apparent (*arrows*). Findings are consistent with a prominent column of Bertin (pseudomass).

Oncocytoma

Renal oncocytomas are benign, solid parenchymal tumors with a reported incidence of approximately 3%–7% among primary renal neoplasms [18]. Medical imaging has been relatively limited in its ability to distinguish oncocytoma and malignant solid renal masses. Due to a high degree of overlap in the imaging characteristics of oncocytomas and low-grade malignant renal neoplasms, surgical resection is frequently performed.

Conventional ultrasound of oncocytomas generally demonstrates a circumscribed, solid renal mass. In a

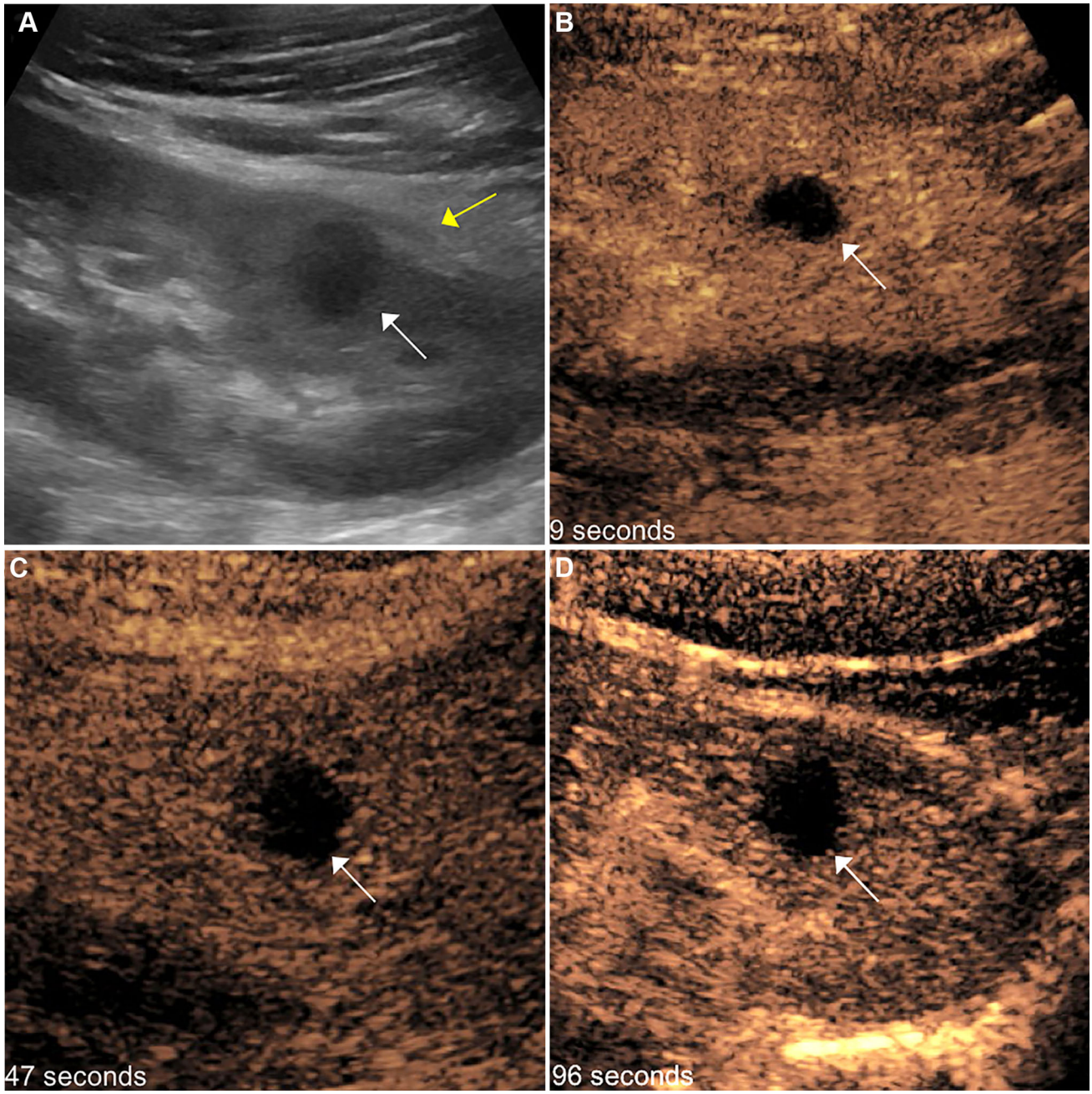

Fig. 10. A 28-year-old female with left costovertebral angle tenderness. **A** Grayscale sonographic image of the left kidney demonstrates a thick-walled cystic lesion at the lower pole (*white arrow*) with low-level internal echoes and perirenal inflammatory changes (*yellow arrow*). **B** CEUS image in the arterial phase (9 s) shows that this cystic lesion is non-enhancing (*arrow*). **C** In the venous phase (47 s), this lesion remains non-enhancing (*arrow*). **D** There is continued non-enhancement (*arrow*) in the delayed phase (96 s). Imaging findings and clinical symptoms were consistent with a renal abscess. Follow-up ultrasound after antibiotic treatment demonstrated resolution of the lesion.

study by Goiney et al. sonographic features suggesting oncocytoma included homogeneous echogenicity, a well-defined margin, size <5.5 cm, and isoechogenicity to the renal parenchyma [19]. However, the utility of these findings is limited, as small RCCs can have similar features. Larger lesions in this study had a more heterogeneous appearance, with areas of necrosis, calcification, or a central stellate scar. Quinn et al. reported that a sonographic central scar was seen in only 25% of oncocytomas [20]. A spoke wheel pattern of vascularity has been reported with oncocytoma, although this finding is typically made at angiography.

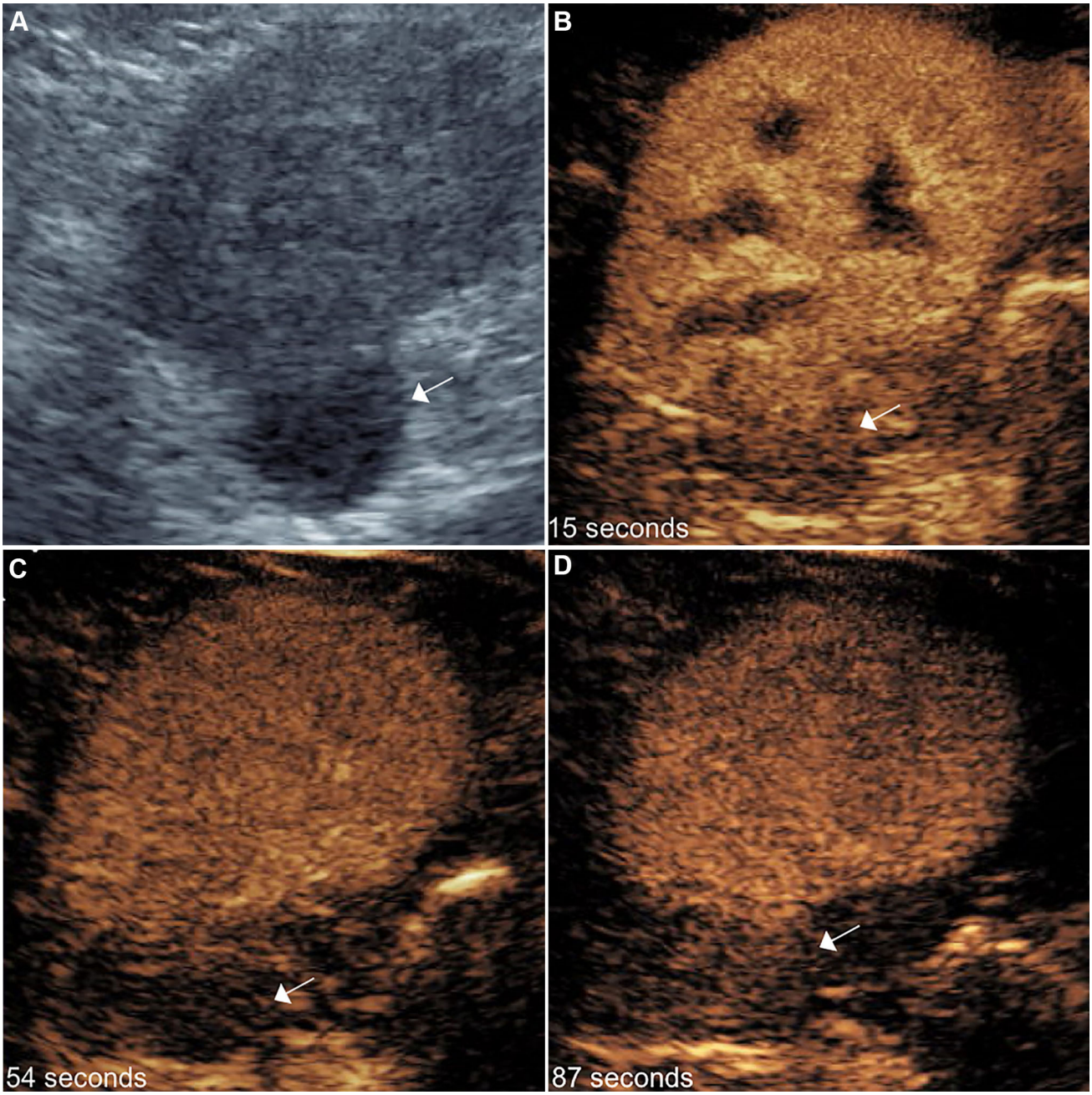

Fig. 11. A 45-year-old male with right renal mass detected on CT urogram. **A** Grayscale ultrasound image of the right kidney demonstrates a round, hypoechoic, exophytic mass at the upper pole (*arrow*). **B** CEUS obtained in the arterial phase (15 s) demonstrates mild enhancement of this mass to a lesser degree than the background renal parenchyma (*arrow*). **C** In the venous phase (54 s), this mass remains hypoenhancing to the renal cortex (*arrow*). **D** There is continued hypoenhancement (*arrow*) in the delayed phase (87 s). Percutaneous biopsy of this lesion yielded B cell lymphoma.

Similar difficulty in distinguishing oncocytomas from RCC has been noted with CT. Davidson et al. showed that the CT features traditionally thought to suggest benignity, such as a central stellate scar and homogeneous enhancement, do not reliably discriminate between oncocytoma and RCC [21]. In a study by Choudhary et al., the degree of lesion enhancement relative to the renal cortex, the presence of a central scar, and the size of a lesion were not reliable CT determinants of oncocytoma [22]. Young et al. reported that both clear cell RCCs and oncocytomas showed peak CT enhancement in the corticomedullary phase, but the magnitude of

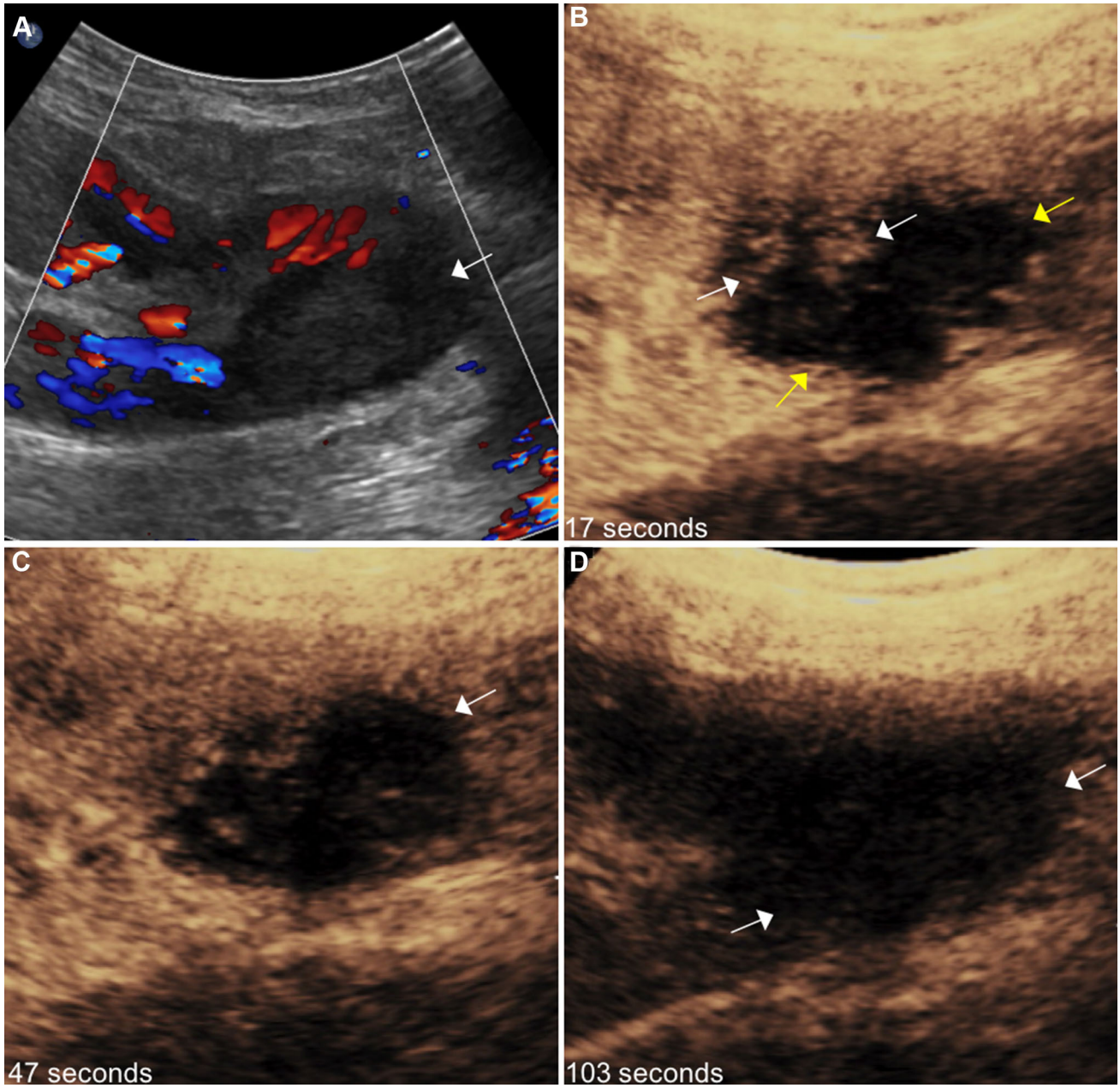

Fig. 12. A 77-year-old male with history of right iliac fossa renal transplant. **A** Color Doppler ultrasound image demonstrates a round, hypoechoic mass at the lower pole of the transplant kidney without significant internal vascularity (*arrow*). **B** CEUS obtained in the arterial phase (17 s) demonstrates this mass to be predominantly hypoenhancing (*yellow arrows*), with a few peripheral nodular areas enhancing to a lesser degree than the background renal parenchyma (*white arrows*). **C** In the venous phase (47 s), this mass remains hypoenhancing to the renal cortex (*arrow*). **D** There is continued hypoenhancement (*arrows*) in the delayed phase (103 s). This lesion underwent percutaneous biopsy and ultimately partial nephrectomy, which demonstrated post-transplant lymphoproliferative disorder (PTLD).

enhancement was greater for RCCs than for oncocytomas in the corticomedullary and excretory phases [23]. Using a multiphase CT protocol, their study distinguished clear cell RCC from oncocytoma with an accuracy of 77%.

As with CT, MRI has not yet been demonstrated to confidently distinguish an oncocytoma from RCC. A study by Rosenkrantz et al. compared several MRI characteristics in chromophobe RCC and oncocytoma, including intralesional blood products, lipid content, T2 hyperintensity, the presence of a central scar, and enhancement pattern [24]. They concluded that none of the studied MR characteristics could reliably discriminate between an oncocytoma and chromophobe RCC. Additional studies comparing the MR features of RCC and oncocytoma have had mixed results [25].

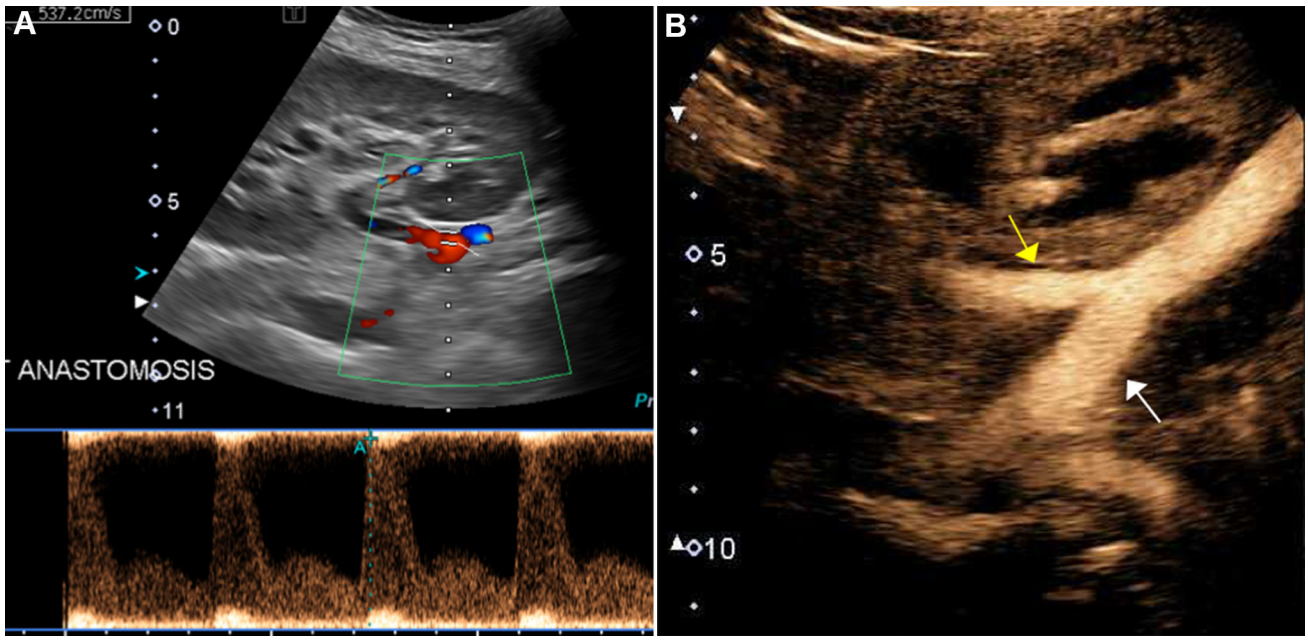

Fig. 13. A 26-year-old male with history of right iliac fossa renal transplant 2 months prior presenting for routine sonographic follow-up. **A** Spectral Doppler evaluation of the transplant kidney demonstrates elevated velocity at the renal artery anastomosis. **B** CEUS of the renal artery anastomosis reveals patent iliac (*white arrow*) and main renal (*yellow arrow*) arteries, without discrete focal narrowing identified. Subsequent laboratory values over the following year demonstrated stable normal renal function in this patient.

CEUS evaluation of oncocytomas is somewhat limited by the small sample size in the available literature. The data are variable, and, as with CT and MRI, there has been no consistent feature on CEUS that can confidently discriminate between oncocytoma and solid RCC. For example, Gerst et al. showed that two out of the three oncocytomas studied were hyperenhancing relative to the renal parenchyma and demonstrated delayed washout, while the third oncocytoma demonstrated a spoke wheel pattern of enhancement, a central scar, and delayed enhancement [26]. In contrast, all five oncocytomas evaluated by Wu et al. demonstrated early arterial hyperenhancement with central progression, a thin peripheral enhancing rim, and rapid washout [27]. Both oncocytomas evaluated by Tamai et al. were hypervascular on CT and CEUS, and one demonstrated spoke wheel enhancement [28]. The retrospective CEUS study by Barr et al. classified three oncocytomas as malignant (false-positive), reinforcing the commonly accepted view that oncocytomas can only confidently be diagnosed at surgical resection [5].

Pseudotumors

A pseudotumor, or pseudomass, refers to a benign renal lesion that mimics a neoplastic process on imaging studies. While this typically represents a developmental variant, the definition is sometimes expanded to include other benign etiologies that can resemble neoplasms, such as vascular, granulomatous, and infectious processes [29]. Examples of developmental variants that can present as pseudotumors include a hypertrophied column of Bertin, dromedary hump, persistent fetal lobulation, and cross-fused renal ectopia.

In many cases, grayscale and Doppler ultrasound are sufficient to diagnose a pseudotumor. Sonographic features supportive of a pseudotumor include isoechogenicity to the renal parenchyma with a similar vascular pattern on Doppler. However, when the diagnosis is unclear by sonography, additional evaluation with CT, MRI, or nuclear medicine studies may be necessary.

CEUS has been shown to be helpful in differentiating between renal pseudotumors and true renal lesions. As would be expected, renal pseudotumors show similar contrast enhancement to the renal cortex on CEUS [13] (Fig. 9). Ascenti et al. used CEUS to evaluate four patients with pseudotumors that were indeterminate by grayscale and power Doppler ultrasound [30]. The presence of smoothly branching vessels extending from the hilum to the periphery, similar to that of adjacent the normal renal cortex, supported a diagnosis of pseudotumor on CEUS.

A study by Mazziotti et al. retrospectively reviewed the CEUS exams of 24 patients with pseudotumors that were indeterminate on conventional and power Doppler

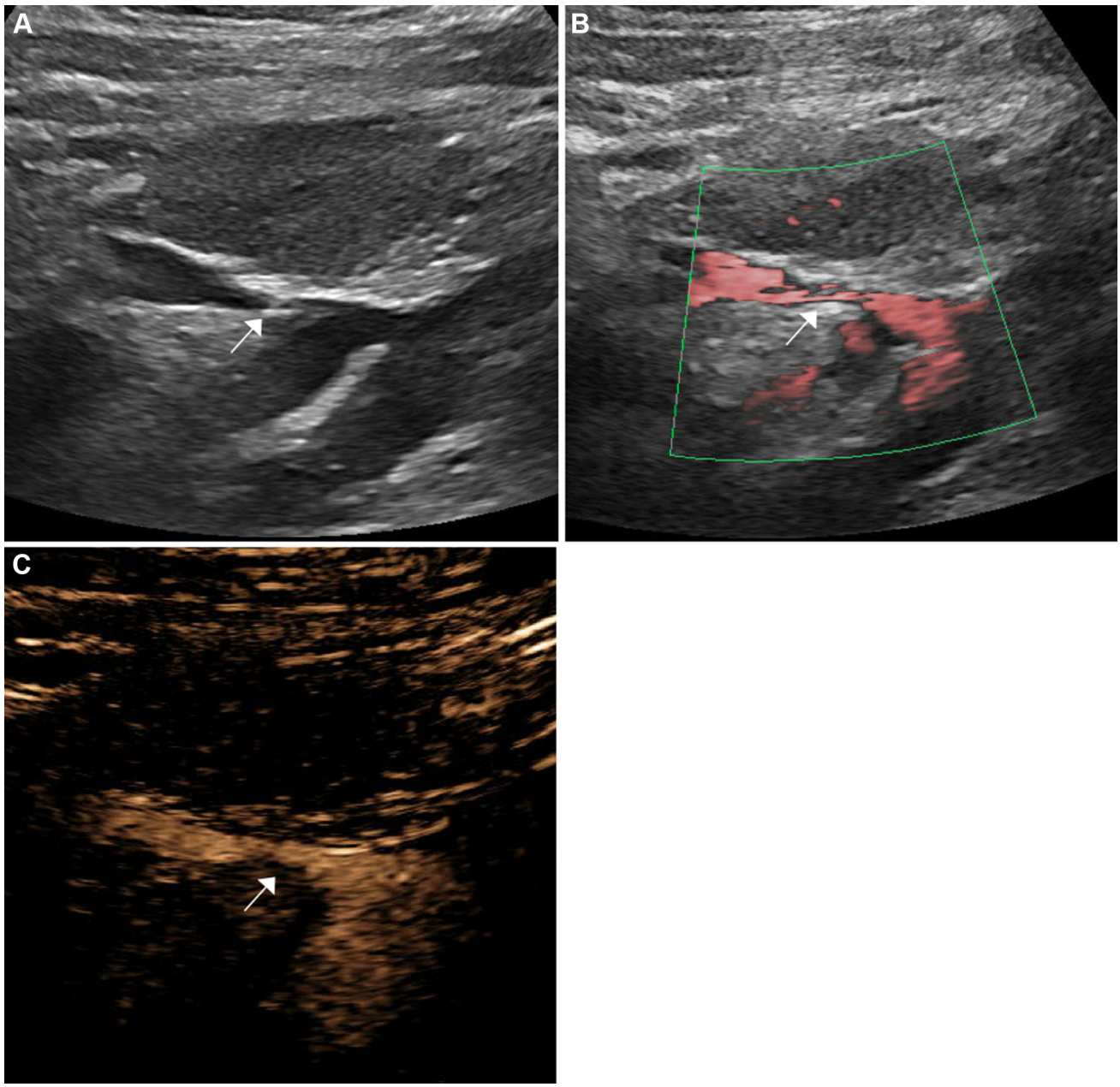

Fig. 14. A 38-year-old male with history of left iliac fossa renal transplant. **A** Grayscale sonographic image of the transplant kidney demonstrates focal narrowing of the distal main renal vein (*arrow*) just proximal to the venous anastomosis. **B** Power Doppler image also demonstrates focal narrowing of the main renal vein distally (*arrow*). **C** CEUS in the venous phase shows corresponding decreased caliber of the vein in this region (*arrow*). Combined grayscale, Doppler, and CEUS findings were concerning for stenosis of the distal renal vein.

ultrasound. In all 24 patients, CEUS was concordant with CT and MRI in characterizing the lesions as benign pseudotumors [31]. Barr et al. used CEUS to evaluate a total of 1018 indeterminate renal lesions in 718 patients [5]. A lesion was classified as a pseudotumor if it enhanced similarly to the background renal cortex on all phases and if a medullary pyramid was detected within the area of concern. CEUS was shown to accurately characterize pseudotumors in this study.

Infection

Infections of the genitourinary tract are frequently encountered within the medical field, accounting for 100,000 hospitalizations and 7 million office visits annually [32]. The diagnosis of a urinary tract infection is usually apparent based on the patient's clinical presentation and laboratory findings, and medical imaging is not required in uncomplicated cases. However, imaging studies are sometimes obtained to evaluate for potential

etiologies of infection, such as an obstructing ureteral calculus or anatomical variant. Additionally, imaging can be helpful to exclude complications like renal abscess formation and perirenal extension of infection, particularly in susceptible patient populations (for example, the immunocompromised, elderly, and diabetics).

CECT is often the initial imaging modality employed to evaluate patients with suspected urinary tract infection. CT findings supporting pyelonephritis include renal enlargement, perirenal inflammatory changes, and heterogeneous attenuation of the kidney [33]. Non-contrast images are sensitive for detecting renal or ureteral calculi, while contrast-enhanced sequences can reveal heterogeneous enhancement and the presence of renal abscesses. Identification of gas within the collecting system or renal parenchyma is also easily assessed with CT.

There is no doubt that CECT is an effective imaging modality for evaluating pyelonephritis and its complications. However, with the high incidence of urinary tract infections, the amount of radiation exposure to the population is not insignificant. This is particularly important when considering the frequency of urinary tract infections in young female patients of childbearing age. Conventional ultrasound can demonstrate ill-defined parenchymal changes, hydronephrosis, and abscess formation. With color and power Doppler, there can be relative hypoperfusion of the involved renal parenchyma. However, conventional ultrasound is overall less sensitive than CT and can miss subtle or early findings in urinary tract infections.

CEUS is emerging as an alternative imaging modality in the evaluation of urinary tract infections. Mitterberger et al. showed nearly equal sensitivity and specificity for CEUS and CT in detecting parenchymal changes associated with pyelonephritis [34]. Findings on CEUS suggestive of pyelonephritis include wedge-shaped perfusion defects and heterogeneous enhancement, similar to what is seen on CT but without the radiation exposure.

In a retrospective study, Fontanilla et al. looked at 48 patients with complicated acute pyelonephritis. Patients were evaluated in the cortical phase (15–30 s following contrast injection), the early parenchymal phase (25 s to 1 min), and the late parenchymal phase (1–4 min) [35]. They found that focal pyelonephritis presented as a wedge-shaped or round hypoenhancing area, best seen in the late parenchymal phase. Renal abscesses, on the other hand, demonstrate central non-enhancement on all sequences (Fig. 10).

Neoplasms of non-renal origin

While less common than primary renal malignancies, metastatic disease to the kidney does occur. Melanoma and cancers of lung, colorectal, and breast origin are the primary malignancies most likely to metastasize to the kidney [36]. In the case of lymphoma, renal involvement is much more likely to be secondary than primary. A study by Honda et al. looked at the CT imaging characteristics of RCC and metastases to the kidney. When compared with RCC, renal metastases were more likely to be bilateral, were smaller in size, demonstrated a wedge-shaped growth pattern, and were less likely to be exophytic [37].

In comparison to RCC and other primary renal lesions, relatively few studies in the literature have looked at CEUS in the setting of renal lymphoma and metastasis to the kidney. There have been reports that these lesions are hypovascular on all CEUS phases [38], which correlates with our experience (Fig. 11).

Renal transplant evaluation

Renal transplant patients are at higher risk of developing carcinoma due to prolonged immunosuppression [39]. Although cysts can occur, careful evaluation of the renal allograft should be made to detect lesions with suspicious features. Transplant patients with gross hematuria or glomerulopathy will typically undergo ultrasound as the initial imaging modality. CT may be obtained if an abnormality is seen on ultrasound. In the presence of a new solid or complex cystic mass, RCC must be excluded. However, post-transplant lymphoproliferative disorder (PTLD) and hemorrhagic cysts can have a similar appearance. The recognition of PTLD is important as there are implications for whether immunosuppressive therapy is altered or ceased (Fig. 12).

Percutaneous biopsy can be performed to determine the etiology of a mass within a transplant kidney. However, as with masses in native kidneys, CEUS can provide additional information about the nature of a lesion. The presence of thickened, nodular septations, and solid components increases the level of suspicion for malignancy. Conversely, CEUS can prove that there is no enhancement within a lesion, indicating that intralesional echoes likely represent hemorrhage or debris.

CEUS can be utilized to assess overall blood flow to a transplant kidney. For example, if the allograft does not enhance or lacks peripheral cortical or regional enhancement, this may indicate an inflow or outflow problem. The transplant renal vasculature can also be assessed with CEUS (Figs. 13, 14).

Biopsy

In cases where a renal mass requires tissue sampling, CEUS can be of value in directing the biopsy needle to the most vascular parts of the lesion. Targeting the enhancing regions of a lesion can help to decrease the non-diagnostic rate by avoiding non-enhancing, potentially necrotic components.

Conclusion

CEUS is a relatively new imaging technique that possesses unique advantages over traditional imaging modalities and can play a vital role in the characterization of indeterminate renal lesions. The dynamic enhancement pattern of a renal mass can be observed under real-time imaging, providing additional information about the nature of a lesion. CEUS does not employ ionizing radiation, it can be performed quickly and at the bedside, and it does not involve administration of potentially nephrotoxic contrast agents. The ability of CEUS to assess the presence of suspicious characteristics within a renal lesion can save tremendous time and resources and can appropriately guide the next step in management. CEUS has also demonstrated value in transplant kidney evaluation and guiding percutaneous biopsies of renal masses.

Compliance with ethical standards

Funding None.

Conflict of interest Brittany Kazmierski declares that she has no conflict of interest. Corinne Deurdulian declares that she has no conflict of interest. Hisham Tchelepi has received research Grants from General Electric and CIVCO Medical Solutions. Edward Grant has received a research Grant from General Electric.

Ethical approval This article does not contain any studies with human participants or animals performed by any of the authors.

References

1. Hollingsworth JM, Miller DC, Daignault S, Hollenbeck BK (2006) Rising incidence of small renal masses: a need to reassess treatment effect. J Natl Cancer Inst 98(18):1331–1334
2. Jinzaki M, Tanimoto A, Mukai M, et al. (2000) Double-phase helical CT of small renal parenchymal neoplasms: correlation with pathologic findings and tumor angiogenesis. J Comput Assist Tomogr 24(6):835–842
3. Li X, Liang P, Guo M, et al. (2013) Real-time contrast-enhanced ultrasound in diagnosis of solid renal lesions. Discov Med 16(86):15–25
4. Xu ZF, Xu HX, Xie XY, et al. (2010) Renal cell carcinoma: real-time contrast-enhanced ultrasound findings. Abdom Imaging 35(6):750–756
5. Barr RG, Peterson C, Hindi A (2014) Evaluation of indeterminate renal masses with contrast-enhanced US: a diagnostic performance study. Radiology 271(1):133–142
6. King KG, Gulati M, Malhi H, et al. (2015) Quantitative assessment of solid renal masses by contrast-enhanced ultrasound with time–intensity curves: how we do it. Abdom Imaging 40(7):2461–2471
7. McGuire BB, Fitzpatrick JM (2010) The diagnosis and management of complex renal cysts. Curr Opin Urol 20(5):349–354
8. Bosniak MA (1986) The current radiological approach to renal cysts. Radiology 158(1):1–10
9. Hartman DS, Choyke PL, Hartman MS (2004) From the RSNA refresher courses: a practical approach to the cystic renal mass. Radiographics 24(Suppl 1):S101–S115
10. Israel GM, Hindman N, Bosniak MA (2004) Evaluation of cystic renal masses: comparison of CT and MR imaging by using the Bosniak classification system. Radiology 231(2):365–371
11. Park BK, Kim B, Kim SH, et al. (2007) Assessment of cystic renal masses based on Bosniak classification: comparison of CT and contrast-enhanced US. Eur J Radiol 61(2):310–314
12. Quaia E, Bertolotto M, Cioffi V, et al. (2008) Comparison of contrast-enhanced sonography with unenhanced sonography and contrast-enhanced CT in the diagnosis of malignancy in complex cystic renal masses. Am J Roentgenol 191(4):1239–1249
13. Ascenti G, Mazziotti S, Zimbaro G, et al. (2007) Complex cystic renal masses: characterization with contrast-enhanced US. Radiology 243(1):158–165
14. Harvey C, Alsafi A, Kuzmich S, et al. (2015) Role of US contrast agents in the assessment of indeterminate solid and cystic lesions in native and transplant kidneys. Radiographics 35(5):1419–1430
15. Forman HP, Middleton WD, Melson GL, McClennan BL (1993) Hyperechoic renal cell carcinomas: increase in detection at US. Radiology 188(2):431–434
16. Jinzaki M, Tanimoto A, Narimatsu Y, et al. (1997) Angiomyolipoma: imaging findings in lesions with minimal fat. Radiology 205(2):497–502
17. Xu ZF, Xu HX, Xie XY, et al. (2010) Renal cell carcinoma and renal angiomyolipoma: differential diagnosis with real-time contrast-enhanced ultrasonography. J Ultrasound Med 29(5):709–717
18. Dechet CB, Bostwick DG, Blute ML, et al. (1999) Renal oncocytoma: multifocality, bilateralism, metachronous tumor development and coexistent renal cell carcinoma. J Urol 162(1):40–42
19. Goiney RC, Goldenberg L, Cooperberg PL, et al. (1984) Renal oncocytoma: sonographic analysis of 14 cases. Am J Roentgenol 143(5):1001–1004
20. Quinn MJ, Hartman DS, Friedman AC, et al. (1984) Renal oncocytoma: new observations. Radiology 153(1):49–53
21. Davidson AJ, Hayes WS, Hartman DS, McCarthy WF, Davis CJ Jr (1993) Renal oncocytoma and carcinoma: failure of differentiation with CT. Radiology 186(3):693–696
22. Choudhary S, Rajesh A, Mayer NJ, Mulcahy KA, Haroon A (2009) Renal oncocytoma: CT features cannot reliably distinguish oncocytoma from other renal neoplasms. Clin Radiol 64(5):517–522
23. Young JR, et al. (2013) Clear cell renal cell carcinoma: discrimination from other renal cell carcinoma subtypes and oncocytoma at multiphasic multidetector CT. Radiology 267(2):444–453
24. Rosenkrantz AB, Hindman N, Fitzgerald EF, et al. (2010) MRI features of renal oncocytoma and chromophobe renal cell carcinoma. Am J Roentgenol 195(6):W421–W427
25. Kang SK, Huang WC, Pandharipande PV, et al. (2014) Solid renal masses: what the numbers tell us. Am J Roentgenol 202(6):1196–1206
26. Gerst S, Hann LE, Li D, et al. (2011) Evaluation of renal masses with contrast-enhanced ultrasound: initial experience. Am J Roentgenol 197(4):897–906
27. Wu Y, Du L, Li F, et al. (2013) Renal oncocytoma: contrast-enhanced sonographic features. J Ultrasound Med 32(3):441–448
28. Tamai H, Takiguchi Y, Oka M, et al. (2005) Contrast-enhanced ultrasonography in the diagnosis of solid renal tumors. J Ultrasound Med 24(12):1635–1640
29. Bhatt S, MacLennan G, Dogra V (2007) Renal pseudotumors. Am J Roentgenol 188(5):1380–1387
30. Ascenti G, Zimbaro G, Mazziotti S, et al. (2001) Contrast-enhanced power Doppler US in the diagnosis of renal pseudotumors. Eur Radiol 11(12):2496–2499
31. Mazziotti S, Zimbaro F, Pandolfo A, et al. (2010) Usefulness of contrast-enhanced ultrasonography in the diagnosis of renal pseudotumors. Abdom Imaging 35(2):241–245
32. Foxman B (2002) Epidemiology of urinary tract infections: incidence, morbidity, and economic costs. Am J Med 113(Suppl 1):5–13
33. Demertzis J, Menias CO (2007) State of the art: imaging of renal infections. Emerg Radiol 14:13–22
34. Mitterberger M, Pinggera GM, Colleselli D, et al. (2007) Acute pyelonephritis: comparison of diagnosis with computed tomography and contrast enhanced ultrasonography. BJU Int 101(3):341–344
35. Fontanilla T, Minaya J, Cortés C, et al. (2012) Acute complicated pyelonephritis: contrast-enhanced ultrasound. Abdom Imaging 37(4):639–646
36. Morichetti D, Mazzucchelli R, Lopez-Beltran A, et al. (2009) Secondary neoplasms of the urinary system and male genital organs. BJU Int 104(6):770–776

37. Honda H, Coffman CE, Berbaum KS, Barloon TJ, Masuda K (1992) CT analysis of metastatic neoplasms of the kidney. Comparison with primary renal cell carcinoma. Acta Radiol 33(1):39–44
38. Ignee A, Straub B, Schuessler G, Dietrich CF (2010) Contrast enhanced ultrasound of renal masses. World J Radiol 2(1):15–31
39. Penn I, Brunson ME (1988) Cancers after cyclosporine therapy. Transplant Proc 20(suppl 3):885–892